IEEE Photonics Journal
An IEEE Photonics Society Publication

Application of A Frequency Chirped RF Intensity Modulated 532 nm Light Source in Underwater Ranging

Volume 12, Number 5, October 2020

Kun Li
Suhui Yang
Yingqi Liao
Xuetong Lin
Xin Wang
Jinying Zhang
Zhuo Li

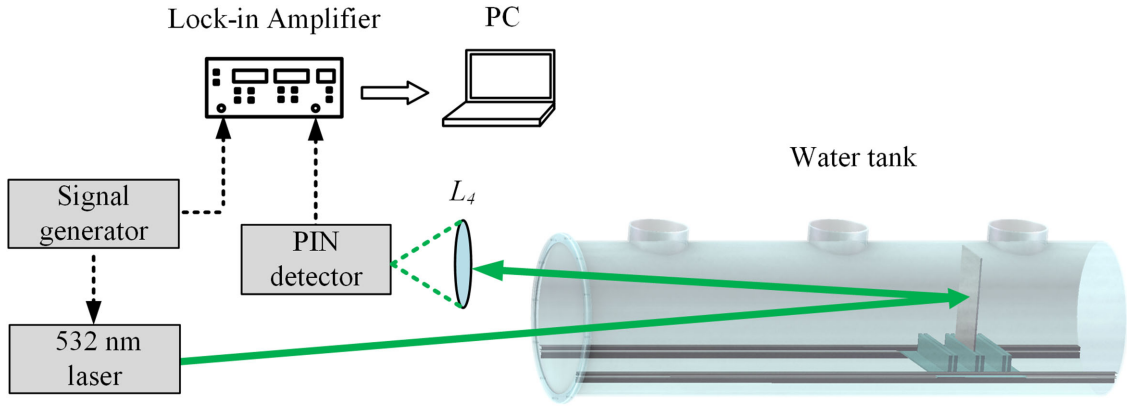

DOI: 10.1109/JPHOT.2020.3024106

Application of A Frequency Chirped RF Intensity Modulated 532 nm Light Source in Underwater Ranging

Kun Li,[1,2,3] **Suhui Yang**,[1,2] **Yingqi Liao**,[1,2] **Xuetong Lin**,[1,2] **Xin Wang**,[1,2] **Jinying Zhang**,[1,2] **and Zhuo Li**[1,2]

[1]School of Optics and Photonics, Beijing Institute of Technology, Beijing 100081, China
[2]Beijing Key Lab. for Precision Optoelectronic Measurement Instrument and Technology, Beijing 100081, China
[3]Kunming Institute of Physics, Kunming 650223, China

DOI:10.1109/JPHOT.2020.3024106

Manuscript received September 8, 2020; accepted September 11, 2020. Date of publication September 15, 2020; date of current version October 2, 2020. This work was supported by the National Nature Science Foundation of China under Grants 61835001, 61875011. Corresponding author: Suhui Yang (e-mail: suhuiyang@bit.edu.cn).

Abstract: A radio-frequency (RF) intensity-modulated light source at 532 nm was built for underwater ranging. The intensity of a narrow-linewidth laser at 1064 nm was modulated via a Mach-Zehnder electro-optical modulator. The modulation frequency could be tuned from 10 MHz to 2.1 GHz. The intensity-modulated light was amplified via a 2-stage laser diode-pumped Yb^{3+} doped large-mode-area fiber amplifier. A 15 mm long magnesium oxide doped periodically-poled lithium niobate (MgO: PPLN) nonlinear crystal was used to convert the 1064 nm light into 532 nm light via frequency doubling. The maximum output power at 532 nm was 2.56 W, the highest efficiency from the fundamental to second harmonic generation (SHG) was 22.6%. The watt level 532 nm light source was applied in underwater ranging experiments. Frequency domain reflectometry (FDR) was applied to retrieve the distances of the objects to the transmitter in a water tank. When the modulation frequency was tuned from 10 MHz to 200 MHz, we obtained ranging accuracy better than 5 cm and ranging resolution smaller than 0.5 cm at 8.6 attenuation length. Two objects spacing by 0.8 m could be resolved simultaneously. The attenuation length at which the object could be detected was limited by the sensitivity of the silicon photodetector. Moreover, we did not use the full bandwidth of the modulation since the lock-in amplifier adopted for data processing had a bandwidth of 200 MHz. Both ranging distance and resolution can be improved if a photomultiplier tube and a high-speed data sampling board were used. Nevertheless, the experimental results showed that the watt level, broadband intensity modulated light source has great potential in underwater detection in terms of ranging accuracy and resolution.

Index Terms: Laser, underwater ranging, modulation, scattering.

1. Introduction

Underwater lidar has the advantages of processing high spatial resolution and compact structure. One superiority of lidar over sonar is that lidar can be ship-borne, airborne, or even spaceborne. The flexibility of the platform of lidar makes it more efficient for detecting objects in a large area. Therefore, lidar is a suitable tool in the fields of marine resource exploration, offshore topographic mapping, underwater target detection [1]–[4]. However, the absorption and scattering of light in water are big challenges for underwater lidar [5]. Absorption causes the attenuation of the laser

signal, limits the detection distance. Scattering not only brings attenuation but also noises. Strong scattering noise can flood the target information. To reduce the absorption, a wavelength in the blue-green transmission window of water was chosen for lidar [6]. Scattering noises are more difficult to overcome. Several approaches were implemented to mitigate scattering noise, e.g., time gating [7], [8], polarization detection [9], [10], narrowing the field of view of the receiver [11], and modulating the intensity of the detecting beam [12]–[15]. Among all the means mentioned above, detection beam modulation technology was based on the fact that photons reflected by the targets could maintain the intensity modulation information, while photons scattered by particles suspending in turbid water at different distances experienced destructive interference resulting in the average of high-frequency modulation signals, by applying correlation of the returned signal with the modulation signal, the signal-to-noise ratio could be improved [16]. In 2014, Illig D W and his coworker used a 450 nm wavelength semiconductor laser with 50 mW output power as a light source for underwater ranging. The intensity was directly modulated from 50 to 550 MHz. A photomultiplier tube was used as the receiver, they achieved a detection range of 14.4 AL (Attenuation Length) with a distance accuracy of 5.63 cm [17].

However, the detection beam modulation technology for underwater detection is hindered by the lack of appropriate light sources. High-power broadband intensity modulated light source is the key to achieve long-distance, high-precision underwater ranging. The power of directly modulated semiconductor laser in the blue and green spectrum is in the order of hundreds of milliwatt [18], which is far from the power level in practical applications. Frequency doubling of solid-state laser is a promising approach to achieve high power green light with good beam quality. In this paper, we will present a high power, broadband intensity modulated light source at 532 nm. A Mach-Zehnder electro-optical modulator (EOM) was used to modulate the intensity of the output from and a non-planar ring oscillator (NPRO) at 1064 nm, a fiber optical power amplifier boosted the output power of the modulated laser beam to twenty watts. Finally, an oxide doped periodically-poled lithium niobate (MgO: PPLN) crystal converts the near-infrared laser light into green light.

The broadband intensity-modulated green light source was applied in underwater ranging experiments. With a normal silicon photodiode detector, the ranging error of 4.94 cm was obtained at 8.6 AL. Considering the distance is inversely proportional to the power. The noise equivalent power of the PIN detector and the photomultiplier are 20 pw/$\sqrt{}$Hz and 0.01 pw/$\sqrt{}$Hz, respectively. In principle, the range will be improved by 45 times. Two objects at different positions alone the beam path were detected simultaneously. The experimental results show that the light source has great potential applications in underwater lidar.

2. The Light Source

The layout of the light source is shown in Fig. 1. A home-made NPRO was used as the seed laser. A specially cut Nd: YAG crystal forms the resonator of the NPRO. The crystal was put in a magnetic field provided by two pieces of magnets. The orientation of the propagation inside the crystal was determined by the orientations of the facets of the crystal. The non-planar propagation in the magnetic field forced the beam to propagate only in one direction, the spatial hole burning effect was avoided therefore single longitudinal mode oscillation was obtained. NPRO was considered one of the most stable light sources in terms of linewidth and power, it was used in the LIGO system as a master oscillator of the light source [19]. The 1064 nm single-frequency laser output from a NPRO was coupled to a Mach-Zehnder EOM. A 10 MHz to 2.1 GHz frequency chirping signal with the amplitude of 1.2 V was generated by a RF signal source and loaded to the Mach-Zehnder EOM. 1% of the light power from the EOM was directed to a photodetector (PD) to provide a reference signal to a bias controller. Since the light output power from the EOM was limited by the low damage threshold of the fast EOM, a 2-stage ytterbium-doped fiber amplifier (YDFA) was used to amplify the modulated laser power to a maximum of 20 W. The second stage of the fiber amplifier used a Yd^{3+} doped double clade large-mode-area silicon fiber in order to maintain single-mode output after amplification.

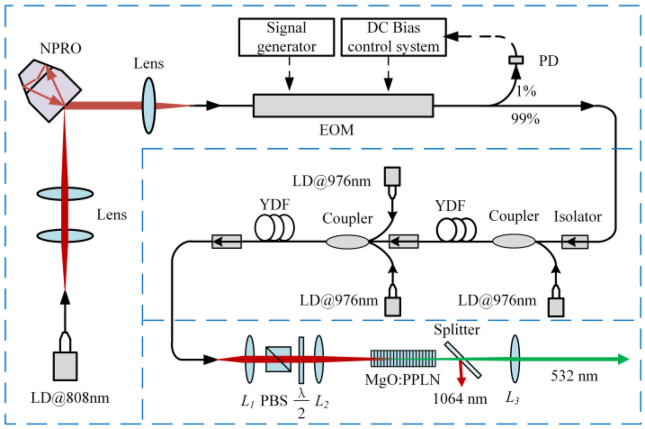

Fig. 1. Layout of the 532 nm broad band intensity modulated light source.

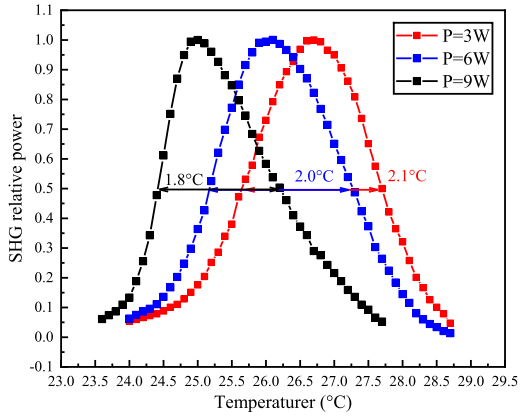

Fig. 2. Bandwidth of phase matching temperature of MgO: PPLN.

The output from the fiber power amplifier was collimated via a lens L_1. A polarizer and a half-wave plate were applied to adjust the polarization direction of the beam to match the polarization direction of the nonlinear crystal. Lens L_2 focused the beam in the middle of the MgO: PPLN crystal installed in an oven. The focal lengths of L_1 and L_2 were 100 mm, 175 mm, respectively. The focused beam in the middle of the nonlinear crystal had a diameter of 44 μm. The output second harmonic generation (SHG) laser was collimated by a lens L_3 with a focal length of 30 mm. The diameter of the collimated green light was about 1 mm and the angle of divergence was 0.5 mrad.

The phase-matching conditions at different pump powers were experimentally investigated. Fig. 2 shows the normalized output power of the SHG as a function of the temperature of MgO: PPLN crystal at different pump powers. As one can see from Fig. 2, the phase matching temperature at higher pump power was lower and the 3 dB phase matching temperature bandwidth was also lower at higher fundamental input power. The temperature bandwidth of the MgO: PPLN crystal were 2.1, 2.0, 1.8 , for the input fundamental power of 3, 6, 9 W, respectively.

Fig. 3 shows the output power and efficiency of the SHG. The highest output power at 532 nm was 2.56 W when the input fundamental power was 11.4 W. The highest efficiency was 22.6%. The phase-matching temperature at each point was adjusted according to the maximum output power of the SHG. The efficiency did not grow linearly with the fundamental input power due to the loss of phase-matching temperature when the fundamental input power increased. Because the thermal conductivity of the nonlinear crystal is rather low, it was very difficult to keep the phase match condition at the whole length of the crystal. When the input power was high, the absorption

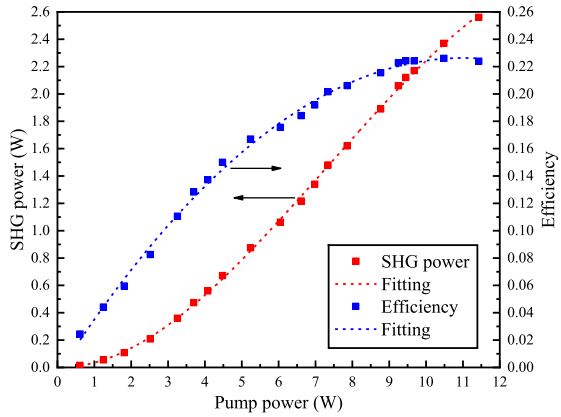

Fig. 3. Output power and energy converting efficiency of SHG at 532 nm.

of the input and SHG light in the crystal caused temperature rising and the phase match condition was lost. Even we adjusted the temperature to get the highest output power, it was still not the perfect phase-matching condition along the whole length in the crystal, the mismatch was getting bigger with the increase of the input power.

The modulation signal applied to the EOM was a frequency chirping signal [20]:

$$f(t) = \cos\left[2\pi\left(f_0 + \frac{B}{T}t\right)t\right], 0 \le t \le T \tag{1}$$

Where f_0 is the initial frequency of the modulation signal, B is the frequency chirping bandwidth, T is the frequency chirping time of period.

The intensity of the modulated laser beam reads:

$$I(t) = \frac{I}{2}[1 + mf(t)] \tag{2}$$

Where m is the modulation index.

The modulated intensity of the SHG then can be expressed from the intensity of the fundamental beam as:

$$\begin{aligned} I_{2\omega}(t) &\propto {I_\omega}^2(t) \\ &= \frac{I^2}{4}[1 + mf(t)]^2 \\ &= \frac{I^2}{4}\left[1 + 2mf(t) + m^2 f(t)^2\right] \\ &= \frac{I^2}{4}\left\{1 + 2m\cos[2\pi(f_0 + \frac{B}{T}t)t] + \frac{m^2}{2}\cos[4\pi(f_0 + \frac{B}{T}t)t] + \frac{m^2}{2}\right\}, 0 \le t \le T \end{aligned} \tag{3}$$

From Eq. (3) one can see, after frequency doubling, the modulation frequency of fundamental beam $f_0 + Bt/T$ can be kept in the SHG. Besides, there is a second harmonic with frequency of $2(f_0 + Bt/T)$ in the modulation spectrum in the SHG beam. The intensity ratio of the second harmonic to the fundamental spectrum in the SHG is:

$$R = \frac{\mathrm{m}^2/2}{2m} = \frac{m}{4} \tag{4}$$

Therefore, the maximum power ratio of the second harmonic component to the fundamental one is 25% when the modulation index is 1.

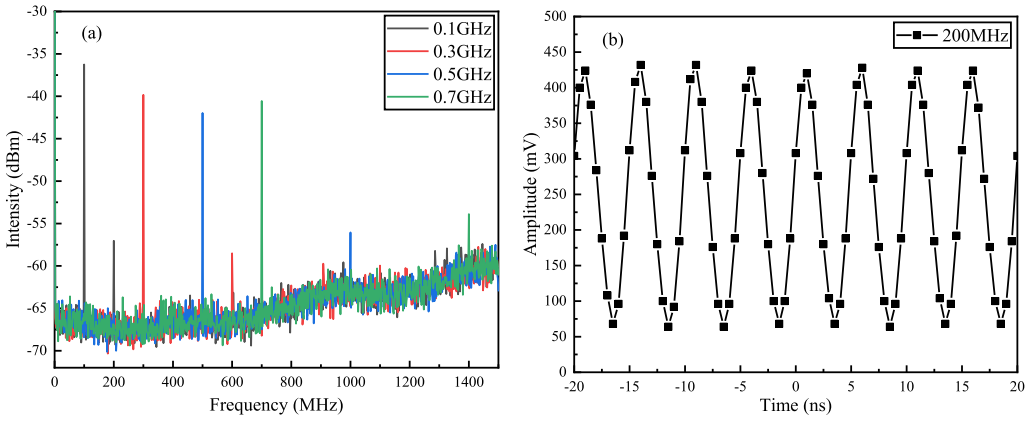

Fig. 4. (a) Modulation spectrum of 532 nm light; (b) Modulation waveform of 532 nm light.

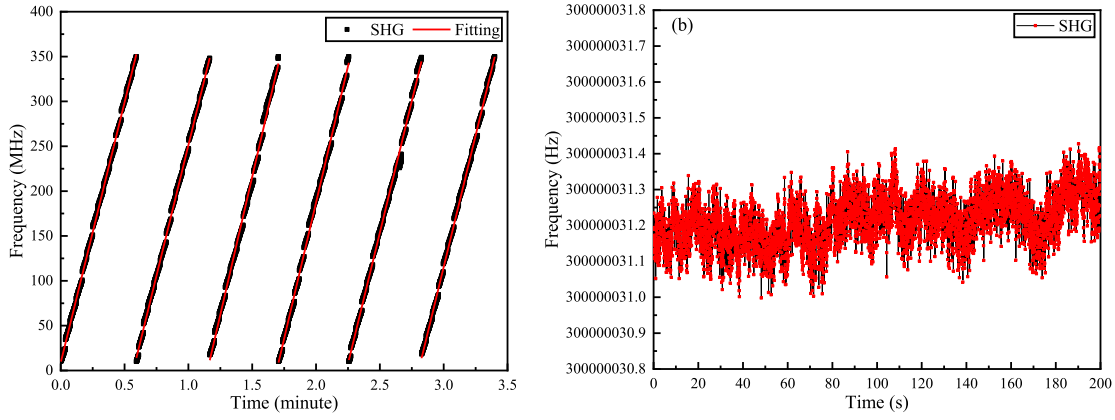

Fig. 5. (a) Frequency sweeping linearity of the modulation; (b) Stability of the frequency of the modulation.

The modulation frequency of the laser can reach 2.1 GHz. Due to the limitation of spectrometer (Siglent, SSA1015X, 9 kHz-1.5 GHz) and detector (CONQUER, KG-PR-1G-AC), the frequency of the modulation signal was set to 0.1, 0.3, 0.5, 0.7 GHz. When the input fundamental power was 0.5 W, we measured the modulation spectra of the SHG, as shown in Fig. 4(a). The modulation frequency of SHG light can not only keep the modulation frequency of pump light, but also produce a second harmonic. The modulation waveform of frequency doubled light was observed by oscilloscope. Fig. 4(b) shows the modulation waveform of the SHG when the modulation frequency was 200 MHz. The modulation index in the SHG was 0.76. High modulation frequency can improve laser ranging resolution. If the bandwidth of the signal source is increased, the modulation frequency of the laser can be higher.

A frequency meter was used to measure the frequency chirping linearity of the modulation in the SHG. Since the bandwidth of the frequency meter was only 350 MHz, we measure the frequency chirping concerning time from 10 MHz to 350 MHz. The step of the frequency measurement was set to 0.1 MHz, at each frequency point, the integration time was set to 10 ms. Fig. 5(a) shows the frequency chirping with respect to time. The linearity was given by the software after the linear fit was done. The linear fit of all the frequency chirping period showed that the linearity of average chirping with time was better than 0.9986. That is to say, the frequency was chirped linearly with time. Fig. 5(b) shows a frequency instability measurement result when the frequency was 300 MHz.

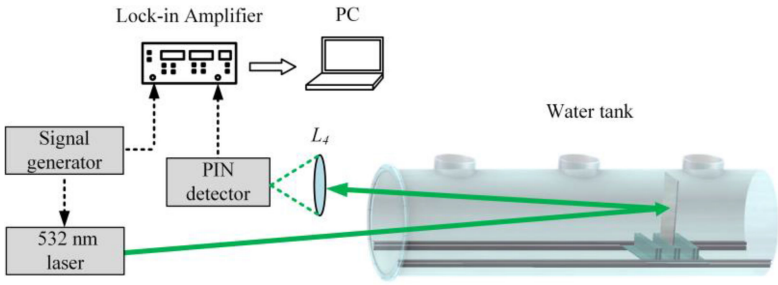

Fig. 6. Experimental setup of underwater ranging.

The frequency instability was less than 0.4 Hz within 200 s of measuring time, the corresponding root means square (RMS) deviation was 0.07 Hz.

3. Underwater Ranging Experiments

3.1 Measurement of the Attenuation Coefficient of Water

The schematic of the experimental setup of underwater ranging is shown in Fig. 6. An object with reflectivity of 0.8 was installed on two rails set in a three meters long water tank. The position of the object could be adjusted through the windows opened on the top of the water tank. $Mg(OH)_2$ powder was put into the water to change the strength of the scattering in the water. The 532 nm light source was installed on an optical bench outside the water tank. The beam was incident to the water through a silicon window. The reflected signal from the target came through the same window and was collected by a lens with a focal length of 50 mm and focused on a fast PIN silicon photodiode detector. A lock-in amplifier was used to sample the signal from the detector. The reference signal to the lock-in amplifier was the signal added to the EOM. Different from conventional optical coherent ranging where a reference beam is needed to have interference signal. The heterodyne detection is done by mixing the electric signals from the detector and drive in the lock-in amplifier. The transverse distance between the transmitting and receiving points were 6 cm, so the angle of the transmitted and reflected beams was neglected when the distance was calculated.

The attenuation of light in water follows Beer-Lambert's law:

$$I(l) = I_0 \exp(-cl) = I_0 \exp(-AL) \tag{5}$$

Where I_0 and $I(l)$ are the intensities of the light at the reference point and after traveling in water for a distance of l, respectively. c is the coefficient of the attenuation in water which includes the attenuation from absorption and scattering. $AL = cl$, is called attenuation length (AL).

We set the positions of the object at two points with distance to the detector of x_1 and x_2, suppose that the light source and detector had the same distance to the object and ignore the difference of the distances between the transmitting and receiving paths. The optical intensity received by the detector can be written as:

$$I_1 = I_0 \alpha^2 \beta \exp(-c \cdot 2x_1) \tag{6a}$$

$$I_2 = I_0 \alpha^2 \beta \exp(-c \cdot 2x_2) \tag{6b}$$

Where, $I_0$is the intensity of the transmitted light outside the water tank, α is the transmission of the silicon window at 532 nm wavelength, β is the albedo of the object. Thus, the attenuation coefficient can be calculated as:

$$c = \frac{\ln(I_1 / I_2)}{2(x_2 - x_1)} \tag{7}$$

TABLE 1
Water Samples With Different Attenuations

Water samples	1	2	3	4
Attenuation coefficients (m^{-1})	0.99	1.72	2.97	4.03

Different amounts of $Mg(OH)_2$ were added into the water tank. We prepared four samples of the water with different attenuation coefficients listed in Table 1.

3.2 Underwater Ranging in Different Water

Frequency domain reflectometry (FDR) was originally developed in the 1980s to detect sharp bends or breaks in fiber and has since found a wide range of applications in which a large unambiguous range and high accuracy are desirable traits [21]. FDR uses a stepped frequency modulation processed by an inverse Fast Fourier Transform (IFFT) to obtain ranging information. In the underwater ranging experiment, a cw optical carrier is modulated by a constant amplitude RF signal with a periodic linear frequency sweep. The detected optical echoes are delayed by propagation in the water to produce a delay in the sweep phase of the modulation. The returned signals are multiplied with the source drive signal in the lock-in amplifier and sampled by a PC. If the sweeping bandwidth is limited, after the inverse Fourier transform (IFT), a corresponding pulse in time domain will be obtained, the pulse width in time domain is inversely proportional to the frequency sweep bandwidth. The pulse position at the time axis corresponds to the delay of the optical signal reflected by the object under the water, which is the information we are interested. FDR was applied since it can improve the signal to noise ration of the detection in an environment with strong scattering noise, like turbid water, and by appropriate data processing, the ranging resolution can be improved.

The modulation frequency was chirped from 50 MHz to 200 MHz with a step $\Delta f = 1$ MHz. The frequency sweeping bandwidth from the light source was much larger but the bandwidth of the lock-in amplifier was only 200 MHz. The lock-in amplifier sampled the amplitude and phase at each frequency point and the data were stored and processed with a PC. By applying inverse fast Fourier transform (IFFT) to the frequency response of the water and target, the position(delay) of the peak of IFFT corresponds to the position of the underwater object. Multiple objects can be detected at the same time with FDR. The unambiguous distance is determined by [17]:

$$d_{UNAMB} = \frac{v}{4\Delta f} \tag{8}$$

Where, v is the velocity of light in water, Δf is the frequency step as mentioned before. In our case, $d_{UNAMB} = 56m$.

The ranging resolution δd in FDR is determined by the frequency sweeping bandwidth, and the points of IFFT n. Theoretically, δd is determined by the following equation:

$$\delta d = \frac{N}{n} * \frac{v}{4B} \tag{9}$$

Where $N = B/\Delta f$ is the number of sampling in the frequency domain. By increasing the points of IFFT which is normally done by zero padding, the ranging resolution can be improved.

We first put the object next to the window, the frequency response was shown in Fig. 7(a). A was the amplitude of the output from the lock-in amplifier, and φ(t) represented the phase of the echoes. Zero padding algorithm was used in IFFT to improve the ranging resolution in the time domain, in which some zeroes were inserted in the frequency axis in the frequency response data [22]. Fig. 7(b) shows the result of IFFT. We inserted 19 points in one frequency bin when we carried out the IFFT, n/N = 20. The peak value of the IFFT appears at a delay of 196.02 ns. We took this position as the origin of the distance of underwater ranging.

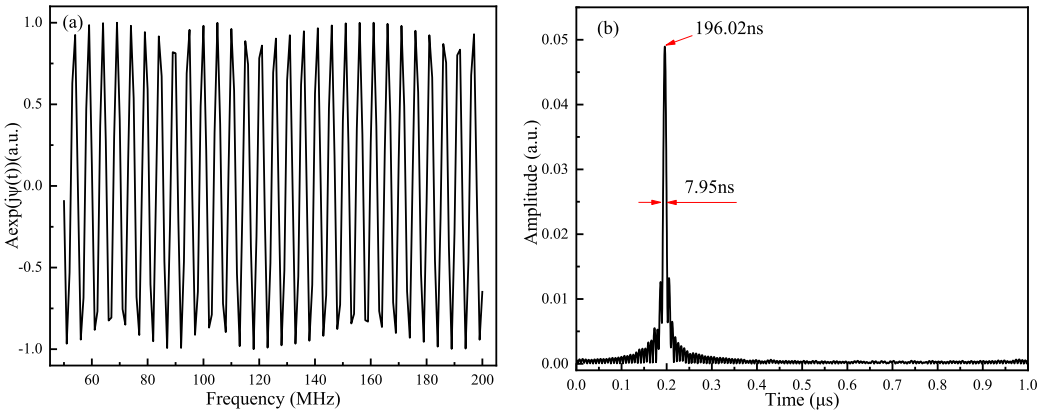

Fig. 7. (a) Frequency response of the target; (b) Diagram of IFFT, the peak position corresponds to the delay time of the reflection from the object.

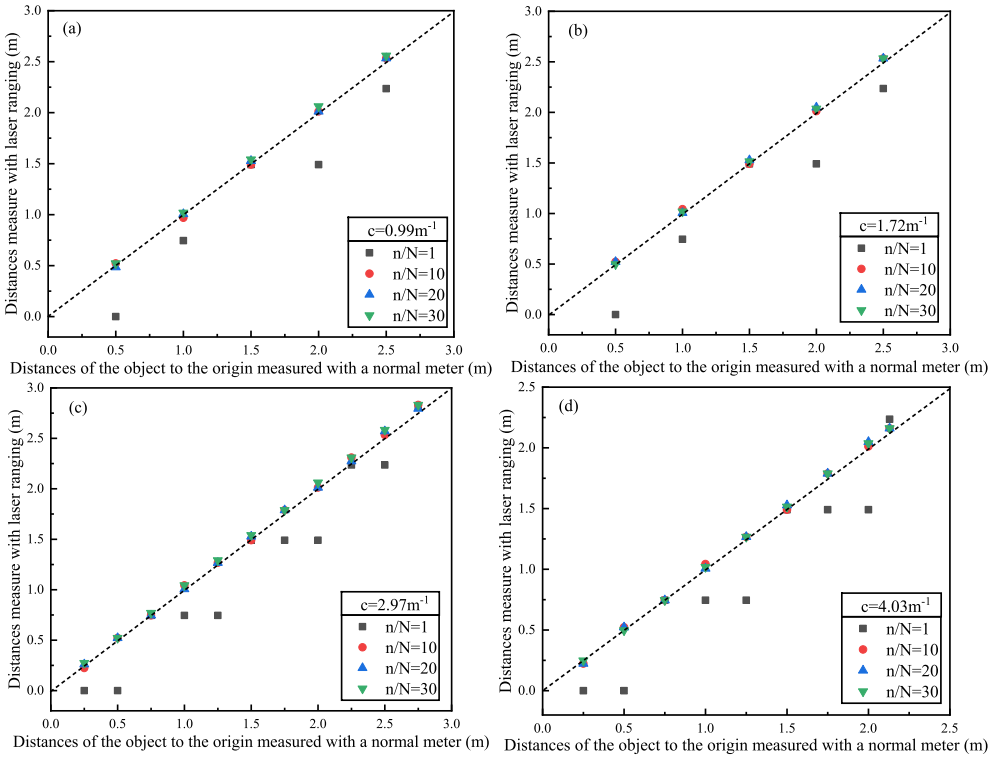

Fig. 8. Ranging results under different attenuation coefficients.

We measured the distance of the object to the window in different turbidities. The results are shown in Fig. 8. The distance of the detected object to the origin was also measured with a normal meter with a minimum scale of mm as shown with the dashed line in Fig. 8. Different numbers of zeroes were inserted into the data when IFFT was applied. When n/N = 1, i.e. no zero was inserted, the raging error was relatively big. With the increase of n/N, the ranging error decreased. When the water became more turbid, the ranging accuracy decreased due to the scattering noise. We reached 8.6 AL when the water attenuation coefficient was 4.03 m^{-1}, the ranging error was

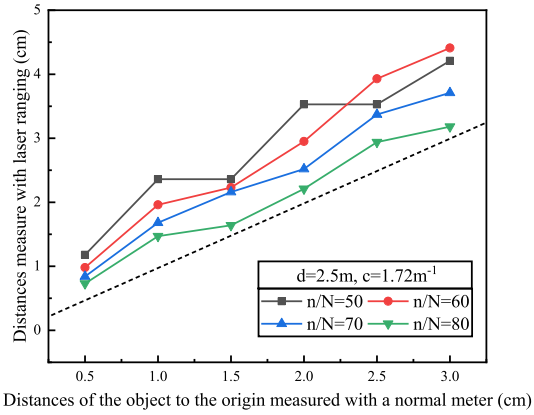

Fig. 9. Ranging resolution of the laser ranging system. (The modulation frequency was 10–200 MHz, the attenuation coefficient of the water was 1.72 m^{-1}).

4.94 cm. The ranging error was the difference between the lidar measurements and the measured values by a meter with the smallest scale of mm.

3.3 Ranging Resolution

In order to test the ranging resolution of the system, the object was moved with small steps to see if the system can resolve the increment. The water attenuation coefficient was 1.72 m^{-1}, the laser modulation frequency was chirped from 10 MHz to 200 MHz with a step of 1 MHz. The object was moved from 2.5 m to the window backward. Each time the object was moved by 0.5 cm. Fig. 9 shows the measured distance with the lidar versus the moving distance of the object. One can see, when the number of zero padding increased, the ranging accuracy also increased. 0.5 cm was well resolved with our setup. If the bandwidth of the light source was fully used, a sub-millimeter of ranging resolution can be expected in rather turbid water.

3.4 Dual Object Raging Simultaneously

We tested the possibility of resolve two objects simultaneously. One object was the quartz window, the other was the plate in the water. The superposition of the reflected signal from the two objects was sampled at the same time and processed with the same method described above. Water with the attenuation coefficient of 0.99 m^{-1} was used. The object was put at 0.5, 0.8, 1.1 m. The thickness of the window was 1 cm, and the refractive index was about 1.461 @ 532 nm. The refractive index of water is 1.333 @ 532 nm, so the window thickness is equivalent to 1.1 cm in water. We put the object at 0.5 m, the frequency response of two object was shown in Fig. 10. The laser reflected from the window of the water tank and the reflected light from the target at 0.5 m incident into the detector at the same time. The amplitude and phase of the echo signal shows modulation after the superposition of the two reflected signals.

When $n/N = 20$, the measurement results are shown in Fig. 11. The distance between the two targets were 0.788, 0.878, and 1.204 m, respectively. When two targets were measured at the same time, in order to separate the two targets accurately, the delay time between the two targets should be longer than the full width at half maximum (FWHM) of the time domain signal after IFFT. Otherwise, the two peak positions of the time domain signals cannot be resolved and the ranging error of the two targets will be big. In this case, the FWHM was 6.28 ns, so only objects with a distance larger than 0.71 m can be resolved simultaneously. When the real distance between the two objects was 0.511 m, the positions of the two peaks were not reliable anymore, so the measurement error was very big. To improve the distance resolution of multiple targets measured

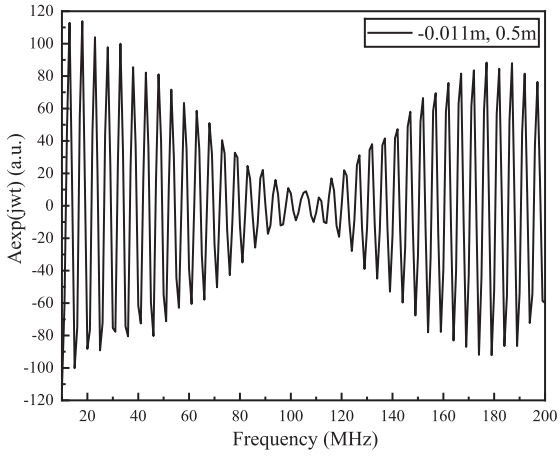

Fig. 10. Frequency response of two targets.

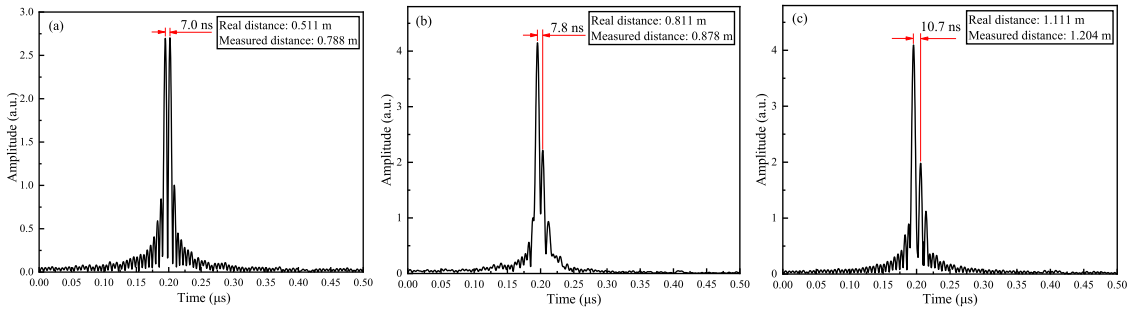

Fig. 11. Ranging results with two targets.

at the same time, the bandwidth of the modulation should be increased. On the other hand, to insert more points in the IFFT data process can also improve the resolution in the time domain.

When two targets are measured at the same time, the long distance between the two targets will cause the reflected signal of the rear target to be submerged in the noise due to the large attenuation. Thus, only the front target can be detected. When the distance between the two targets is close to each other, in order to separate them, the laser source with broad modulation bandwidth is needed to improve the range resolution. The FDR technology can realize the simultaneous measurement of multiple targets in the same direction with a single beam, or targets in different directions after expending the emitted laser beam and illuminating multi targets. When a single beam is used to measure multiple targets in the same direction, the front target should be transparent to some extent so that the beam can reach the rear targets. In the case of expending beam, the laser beam will cover multi targets. The detector receives all the echo signals at the same time. By IFFT, the ranges of multiple targets can be obtained simultaneously. The multiple targets simultaneous measurement can improve the detection efficiency in the target searching. In the scanning detection system, multi-layer simultaneous scanning can be realized, and a three-dimensional image can be obtained.

4. Conclusion

A broadband frequency chirped intensity modulated light source was built for underwater ranging. The modulation frequency was tuned from 10 MHz to 2.1 GHz. The maximum output power was 2.56 W at 532 nm wavelength. The light source was applied in an underwater lidar system. A

PIN silicon photodiode was used to detect reflected signals. Frequency domain reflectometry was applied to resolve the distance of the underwater object to the reference point. Zero padding algorithm was applied in IFFT to increase the ranging resolution. 8.6 AL was reached with a ranging error of less than 4.94 cm. In turbid water with an attenuation coefficient of 1.72 m^{-1}, 0.5 cm ranging resolution was achieved. The ranging resolution was limited by the bandwidth of the data processing unit, this number can be reduced to sub-millimeter if the full chirping bandwidth of the light source was used. Two objects were resolved at the same time. In the future study, a PMT will be used as the detector to increase the sensitivity. We will also increase the bandwidth of the signal processing unit in order to fully benefit the broadband frequency chirping capability of the light source.

References

[1] J. S. Jaffe, "Underwater optical imaging: The past, the present, and the prospects," *IEEE J. Ocean. Eng.*, vol. 40, no. 3, pp. 683–700, Jul. 2015.

[2] Busck and Jens, "Underwater 3-D optical imaging with a gated viewing laser radar," *Opt. Eng.*, vol. 44, no. 11, 2005, Art. no. 116001.

[3] A. Jantzi, W. Jemison, A. Laux, L. Mullen Jemison, and B. Cochenour, "Enhanced underwater ranging using an optical vortex," *Opt. Express*, vol. 26, no. 3, pp. 2668–2674, 2018.

[4] A. Laux, L. Mullen, P. Perez, and E. Zege, "Underwater laser range finder," in *Proc. SPIE Conf. Ocean Sens. Monit. IV*, 2012, Art. no. 8372.

[5] V. I. Haltrin, "Self-consistent approach to the solution of the light transfer problem for irradiances in marine waters with arbitrary turbidity, depth, and surface illumination. I. Case of absorption and elastic scattering," *Appl. Opt.*, vol. 37, no. 18, pp. 3773–3784, 1998.

[6] S. Q. Duntley, "Light in the Sea," *J. Opt. Soc. Amer.*, vol. 53, no. 2, pp. 214–233, 1963.

[7] E. A. Mclean, H. R. Burris, and M. P. Strand, "Short-pulse range-gated optical imaging in turbid water," *Appl. Opt.*, vol. 34, no. 21, pp. 4343–4351, 1995.

[8] S. Liang *et al.*, "Lower-upper-threshold correlation for underwater range-gated imaging self-adaptive enhancement," *Appl. Opt.*, vol. 55, no. 29, pp. 8248–8255, 2016.

[9] J. Cariou, B. L. Jeune, J. Lotrian, and Y. Guern, "Polarization effects of seawater and underwater targets," *Appl. Opt.*, vol. 29, no. 11, pp. 1689–1695, 1990.

[10] M. Dubreuil, P. Delrot, I. Leonard, A. Alfalou, C. Brosseau, and A. Dogariu, "Exploring underwater target detection by imaging polarimetry and correlation techniques," *Appl. Opt.*, vol. 52, no. 5, pp. 997–1005, 2013.

[11] A. Maccarone, F. M. D. Rocca, A. Mccarthy, R. Henderson, and G. S. Buller, "Three-dimensional imaging of stationary and moving targets in turbid underwater environments using a single-photon detector array," *Opt. Express*, vol. 27, no. 20, pp. 28437–28456, 2019.

[12] L. Mullen, B. Cochenour, A. Laux, and D. Alley, "Optical modulation techniques for underwater detection, ranging and imaging," in *Proc. SPIE Conf. Ocean Sens. Monit. III*, 2011, Art. no. 8030.

[13] L. J. Mullen and V. M. Contarino, "Hybrid LIDAR-radar: Seeing through the scatter," *IEEE Microw. Mag.*, vol. 1, no. 3, pp. 42–48, Sep. 2000.

[14] D. W. Illig, W. D. Jemison, L. Rumbaugh, R. Lee, A. Laux, and L. Mullen, "Enhanced hybrid lidar-radar ranging technique," in *Proc. IEEE Conf. An Ocean Common.*, 2013, pp. 1–9.

[15] S. O'Connor, R. Lee, L. Mullen, and B. Cochenour, "Waveform design considerations for modulated pulse lidar," in *Proc. SPIE Conf. Ocean Sens. Monit. VI*, 2014, Art. no. 9111.

[16] D. W. Illig, W. D. Jemison, R. W. Lee, A. Laux, and L. J. Mullen, "Optical ranging techniques in turbid waters," in *Proc. SPIE Conf. Ocean Sens. Monit. VI*, 2014, Art. no. 9111.

[17] D. W. Illig, L. Rumbaugh, W. D. Jemison, A. Laux, and L. Mullen, "Statistical backscatter suppression technique for a wideband hybrid lidar-radar ranging system," in *Proc. IEEE Conf. Ocean*, 2014, pp. 1–7.

[18] Y. Maegami *et al.*, "High-efficiency strip-loaded waveguide-based silicon Mach-Zehnder modulator with vertical p-n junction phase shifter," *Opt. Express*, vol. 25, no. 25, pp. 31407–31416, 2017.

[19] T. J. Kane, R. L. Byer, "Monolithic, unidirectional single-mode Nd:YAG ring laser," *Opt. Lett.*, vol. 10, no. 2, pp. 65–67, 1985.

[20] A. Samarah, "A 320 MHz digital linear frequency modulated signal generator for radar applications using FPGA technology," in *Proc. IEEE Conf. Comput. Intell. Commun. Netw.*, 2014, pp. 966–972.

[21] R. I. MacDonald, "Frequency domain optical reflectometer," *Appl. Opt.*, vol. 20, no. 10, pp. 1840–1844, 1981.

[22] R. Deka and J. G. Gardiner, *Fundamentals of Digital Signal Processing Using MATLAB*. Xi'an, China: Xi'an Jiaotong University Press, 2005.